Performance Analysis of Amplify-Decode-and-Forward Multihop BPSK/FSO Systems using APD Receivers over Atmospheric Turbulence Channels

Journal:	*IET Communications*
Manuscript ID:	COM-2013-0422.R2
Manuscript Type:	Research Paper
Date Submitted by the Author:	01-Dec-2013
Complete List of Authors:	Pham, Thanh; University of Aizu, Computer Engineering Pham, Anh; The University of Aizu, Computer Engineering
Keyword:	FREE-SPACE OPTICAL COMMUNICATION, RELAY NETWORKS, ATMOSPHERIC LIGHT PROPAGATION
Note: The following files were submitted by the author for peer review, but cannot be converted to PDF. You must view these files (e.g. movies) online.	
0_paper_shorten-revision-final-pham.tex	

Performance Analysis of Amplify-Decode-and-Forward Multihop BPSK/FSO Systems using APD Receivers over Atmospheric Turbulence Channels

Thanh V. Pham and Anh T. Pham

Abstract

This paper studies the performance of multihop free-space optical (FSO) systems using the subcarrier binary phase-shift keying modulation (BPSK) over atmospheric turbulence channels. We propose a modified relaying strategy, termed *amplify-decode-and-forward* (ADF), realised by using avalanche photodiode (APD) receivers. The outage probability of the proposed system is analytically derived considering the atmospheric turbulence and the receiver noise, including APD shot noise and thermal noise. The analytical results are verified by Monte Carlo simulations, and a good agreement between the analytical and simulation results is confirmed. In our analysis, we quantitatively discuss the impact of turbulence strength, number of relay nodes, relaying configuration, system bit rate and receiver parameters on the system outage probability. In addition, the optimal value of APD gain for achieving the lowest outage probability in different cases of relaying configuration, number of relays, and receiver parameters is also discussed.

Index Terms

Free-space optical communications, multihop, atmospheric turbulence, APD receiver, outage probability, log-normal distribution, gamma-gamma distribution.

I. Introduction

Free-space optical (FSO) communications is an optical transmission technology that uses the light signal to transmit data over free space in telecommunications or computer networks. It has recently emerged as one of the important technologies in wireless communications thanks to its significant advantages of high data rates, ease of deployment, license-free and long-range operation [1], [2]. In

Authors are with the Computer Communications Lab., University of Aizu, Fukushima, Japan

addition, the FSO communications also offers an effective solution for the spectrum scarcity problem, especially in the wireless-access environment.

One of the most challenging issues for the realisation of FSO systems, especially over the long distance (more than 2 km), is the effect of atmospheric turbulence, which is caused by the variation of refractive-index of the air [2]. The atmospheric turbulence causes the intensity fluctuation of the received optical signal, which reduces the system performance. Several statistical models have been proposed to describe the atmospheric turbulence in the literature. For the weak-to-moderate turbulence, the log-normal distribution is suitable for modelling the atmospheric channel. On the other hand, the gamma-gamma distribution is generally accepted for the moderate-to-strong turbulence.

In order to increase the reliability as well as to achieve a broader coverage of the FSO systems over atmospheric turbulence channels, multihop (or relaying) transmission technique has been proposed as a potential solution [4]. The main idea of this technique is to relay signal from the source to the destination through intermediate terminals called relay nodes; and depending on the structure of relay nodes, there are two relaying strategies, namely: decode-and-forward (DF) and amplify-and-forward (AF) relaying. In the AF relaying, the received signal at each relay node is amplified before it is retransmitted to the following relay node. In case of the DF relaying technique, the received signal is detected and demodulated to recover the original data before it is regenerated for relaying to the next node.

There has been recently a number of studies on the analysis of the outage probability of multihop FSO systems [5]–[8]. For the log-normal channel, Safari $et\ al.$ [5] derived the outage probability of serial and parallel relay-assisted FSO systems for both AF and DF relaying techniques. Also, Karimi $et\ al.$ presented the outage analysis of parallel relaying with cooperative protocol [6]. The outage analyses of AF and DF relaying systems over the gamma-gamma channel were presented in [7]–[9]. Previous studies reveal that in the FSO communications, due to the complexity and cost of the all-optical amplifying systems [10], the AF relaying is less attractive in comparison with the DF one. In addition, the noise is added to the received signal at each intermediate relay node through transmission path, resulting in the limited transmission distance. The purpose of the DF technique is to eliminate the noise propagation, it therefore greatly improves system performance in comparison with that of the AF technique [5]. On the other hand, it is worth noting that the impact of receiver noise, including the shot noise and thermal noise, is critical in optimizing the design of optical systems, and it has been thoroughly studied in single hop FSO systems [12], [13]. However, to the best of our knowledge, it has not been considered in all previous studies of DF relaying systems.

In this paper, we therefore study the outage behaviour of the multihop FSO systems considering the impact of both the atmospheric turbulence channel and receiver noise in both destination and relay nodes. In addition, we employ a modified DF relaying with amplification, termed *amplify-decode-and-forward* (ADF), which is realised by using avalanche photodiode (APD) receivers at the destination

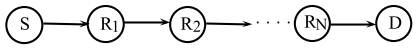

(a) Serial configuration

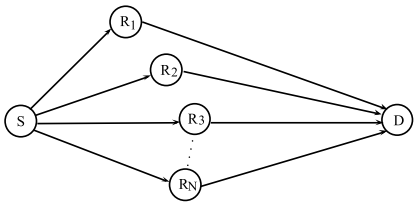

(b) Parallel configuration

Fig. 1: Multihop FSO configurations

and relay nodes. In the ADF relaying, the received signal at each relay node will be amplified and decoded by an APD receiver. The decoded data is then regenerated and forwarded to the following node. The implementation of the proposed ADF systems is basically similar to that of the DF ones; the only difference is that APDs are used instead of p-i-n photodiodes.

Besides the proposal of the modified ADF relaying strategy, another key contribution of the paper is the derivation of closed-form expressions of the system outage probability taking into account both atmospheric turbulence and receiver noise. It is important to note that all previous studies only assumed that noise was signal-independent (which is not practically realistic) so that the closed-form expression derivation was considerably simpler. In addition, we get the closed-form for both serial and parallel configurations over log-normal and gamma-gamma channel models for the cases of weak-to-moderate and moderate-to-strong atmospheric turbulences, respectively. Finally, we validate the analytical results by Monte Carlo simulations and a good agreement between the analytical and simulation results is confirmed.

The rest of the paper is organised as follows. In Section II, we introduce the system model and the serial and parallel relaying configurations. The proposed system using APD receivers and atmospheric turbulence channel models are also described in this section. The outage probability analysis is presented in Section III. Section IV presents the numerical results and discussions. Finally, we conclude the paper in Section V.

II. System Descriptions

A. System Models

We consider a multihop FSO system employing subcarrier binary phase-shift keying modulation (BPSK) signalling, in which there are N relay nodes between the source and the destination node. The BPSK signalling is selected thanks to its use of the “zero” threshold level, which, in comparison with the on-off keying (OOK), results in the easier signal detection in the presence of atmospheric

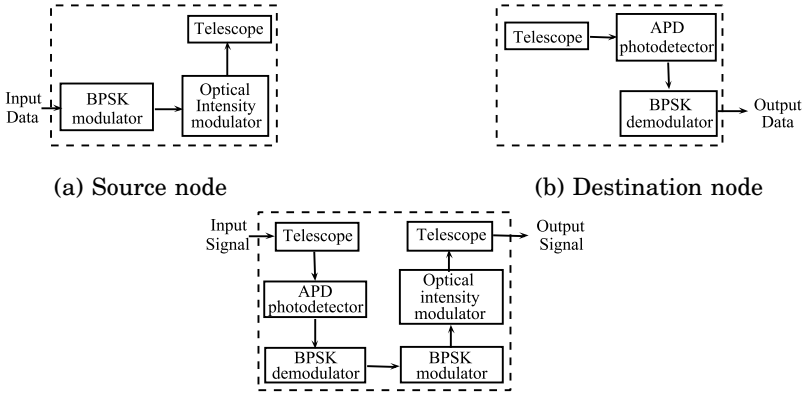

(a) Source node (b) Destination node

(c) Relay nodes

Fig. 2: Architectures of the source, relay and the destination nodes

turbulence [13]. These N nodes can be arranged in either serial or parallel fashion, thus respectively, we have the serial and parallel relaying configurations, as shown in Figs. 1a and 1b.

In both serial and parallel systems, there are three types of nodes: source, destination and relay nodes; and in the ADF mode the architectures of these nodes are illustrated as in Fig. 2, in which APDs are used as photodetector in all DF relay nodes and the destination node. The source node consists of a subcarrier BPSK transmitter, as illustrated in Fig. 2a. Binary data is first electrically modulated onto a radio frequency (RF) subcarrier by the BPSK modulator, by which bit '0' and bit '1' are represented by two different phases 180^0 apart. In the optical intensity modulator, the electrical BPSK signal is used to modulate the intensity of the light source, i.e., a laser beam. The direction and the size of the laser beam are determined by the collimator or telescope in the transmitter. At the destination node, as in Fig. 2b, there is a subcarrier BPSK receiver. The incoming optical field from the telescope is converted into an electrical signal by the APD. The transmitted data is then recovered by using a standard RF coherent demodulator.

At each relay node, there is a pair of subcarrier BPSK transmitter and receiver, as shown in Fig. 2c. The received optical signal is detected, amplified by APD and the data is recovered (i.e., decoded). The decoded data is then re-encoded at the subcarrier BPSK transmitter and relayed to the following node or the destination depending on the configuration (serial or parallel) and the position of the relay node.

B. Channel Models

We first examine a FSO channel between two terminals A and B. The received signal $P(t)$ at terminal B can be expressed as

$$P(t) = aX(t)P_0(t), \tag{1}$$

where $a, X(t), P_0(t)$ denote the channel loss, the random process representing the scintillation caused by atmospheric turbulence and the transmitted signal power, respectively. The channel loss due to both molecular absorption and aerosol scattering suspended in the air, is given by [14]

$$a = \frac{A_r}{\pi\left(\frac{\phi\ell}{2}\right)^2}\exp(-\beta_\nu \ell), \tag{2}$$

where $A_r, \phi, \ell, \beta_\nu$ denote the area of the receiver aperture, the optical beam's divergence angle in radian, the channel distance between two terminals and the atmospheric extinction coefficient, respectively.

The irradiance fluctuations represent the signal scintillation caused by the atmospheric turbulence. When the turbulence is weak, it is generally accepted that $X(t)$ could be modeled as a random process with log-normal distribution. Assuming that the average of the random process $X(t)$ is normalized to unity, its probability density function (pdf) is given by

$$f_X(x) = \frac{1}{\sqrt{2\pi}\sigma_s x}\exp\left[-\frac{(\ln x + \sigma_s^2/2)^2}{2\sigma_s^2}\right]. \tag{3}$$

Here, σ_s^2 is the log intensity variance depending on the channel's characteristics with respect to the distance of two terminals and is given by [15]

$$\sigma_s^2 = \exp\left[\frac{0.49\sigma_s^2}{\left(1+0.18d^2+0.56\sigma_R^{\frac{12}{5}}\right)^{\frac{7}{6}}} + \frac{0.51\sigma_s^2}{\left(1+0.9d^2+0.62d^2\sigma_R^{\frac{12}{5}}\right)^{\frac{5}{6}}}\right] - 1, \tag{4}$$

in which, $d = \sqrt{kD^2/4\ell}$, and $k = 2\pi/\lambda$ is the optical wave number. The parameter σ_R^2 is the Rytov variance, and assuming plane wave propagation, it is given by

$$\sigma_R^2 = 1.23 C_n^2 k^{7/6}\ell^{11/6}, \tag{5}$$

where C_n^2 is the altitude-dependent index of the refractive structure parameter determining turbulence strength.

When turbulence strength becomes stronger (typically, when the value of C_n^2 is greater than 2×10^{-14}), $X(t)$ can be modelled as a random process with gamma-gamma distribution and its pdf is given by [15]

$$f_X(x) = \frac{2(\alpha\beta)^{\frac{\alpha+\beta}{2}}}{\Gamma(\alpha)\Gamma(\beta)}x^{\frac{\alpha+\beta}{2}-1}K_{\alpha-\beta}(2\sqrt{\alpha\beta x}). \tag{6}$$

Here $\Gamma(.)$ is the gamma function, and $K_{\alpha-\beta}(.)$ is the modified Bessel function of the second kind and order $\alpha-\beta$. Beside the link length ℓ, α and β are given by [15]

$$\alpha = \left\{\exp\left[\frac{0.49\sigma_R^2}{\left(1+1.11\sigma_R^{12/5}\right)^{7/6}}\right] - 1\right\}^{-1}, \tag{7}$$

$$\beta = \left\{\exp\left[\frac{0.51\sigma_R^2}{\left(1+0.69\sigma_R^{12/5}\right)^{5/6}}\right] - 1\right\}^{-1}, \tag{8}$$

where σ_R^2 with respect to the distance ℓ between two terminals is given in Eq. (5).

C. Single hop FSO System using APD Receiver

Now we consider a single hop FSO system using APD receiver and subcarrier BPSK signalling. In such system, the received optical power $P(t)$ can be written as

$$P(t) = aX(t)\frac{P_s}{2}[1 + m\cos(2\pi f_c t + b_k\pi)], \tag{9}$$

where P_s is the average transmitted power, m is the modulation index, f_c is the subcarrier frequency, and $b_k \in \{0, 1\}$ denotes the binary data signal.

As the temporal correlation time of the atmospheric scintillation process is on the order of several milliseconds, which is much longer than a bit duration (less than a microsecond when the bit-rate is higher than tens of Mb/s), the dc term $aX(t)P_s/2$ can be filtered out by a bandpass filter. The output electrical signal of the APD therefore can be expressed as

$$I(t) = m\Re\bar{g}\frac{P_s}{2}aX(t)\cos(2\pi f_c t + b_k\pi) + n(t), \tag{10}$$

where $\Re$, $\bar{g}$, $n(t)$ denote the responsivity, the average APD gain and the receiver noise, respectively. For BPSK demodulation, by employing a coherent detection, the output signal $r(t)$ can be written as

$$r(t) = \overline{I(t)\cos(2\pi f_c t)} = \begin{cases} \frac{1}{4}m\Re\bar{g}P_s aX(t) + \xi(t) & \text{in the mark state} \\ -\frac{1}{4}m\Re\bar{g}P_s aX(t) + \xi(t) & \text{in the space state} \end{cases} \tag{11}$$

where $\xi(t)$ is the APD receiver noise including APD shot noise, thermal noise and dark current. Assuming the dark current is negligible, $\xi(t)$ can be given by

$$\xi(t) = i_{Th}(t) + i_{Sh}(t), \tag{12}$$

where $i_{Th}(t)$ and $i_{Sh}(t)$ are the thermal noise and shot noise, respectively. The thermal noise can be modelled as a zero-mean stationary Gaussian random process whose the variance is given by

$$\sigma_{Th}^2 = \frac{4k_B T}{R_L}F_n\Delta f, \tag{13}$$

in which $k_B, T, R_L, F_n, \Delta f$ denote the Boltzmann constant, the absolute temperature of receiver, the APD's load resistance, the amplifier noise figure and the effective noise bandwidth, respectively [16]. The effective noise bandwidth depends on the bit rate, the shapes of received and equalised pulses, and the design of the receiver. We choose the typical $\Delta f = R_b/2$, where R_b is the system bit rate.

Considering the APD shot noise, the scintillation causes the fluctuation in the received optical signal and it also leads to uncertainty in the shot noise variance. Again, as the temporal correlation time is much longer than a bit duration, the scintillation could be considered to be constant during the bit duration. $i_{Sh}(t)$ therefore can be also modelled as a stationary Gaussian random process whose the variance is given by [16]

$$\sigma_{Sh}^2 = 2q\bar{g}^2 F_A\Re\left(\frac{m}{4}P_s ax\right)\Delta f, \tag{14}$$

where q is the electron charge and F_A is the exceed noise factor and given by $F_A = k_A\bar{g} + (1-k_A)(2-\frac{1}{\bar{g}})$, where k_A is the ionisation factor. Finally, as the shot noise and thermal noise are independent Gaussian random processes, the total variance of APD receiver noise can be obtained by adding these individual variances as $\sigma^2 = \sigma_{Sh}^2 + \sigma_{Th}^2$.

D. ADF Multihop FSO System using APD Receivers

In the analysis, we use the indexes 0 and $N+1$ for indicating the source and destination nodes, respectively; the indexes from $1, 2, ...,$ to N are used for the N relay nodes. We also assume that the APD receiver parameters at each node are the same, and the atmospheric fluctuations at all hops are independent and identically distributed. For both relaying configurations, it is assumed that total transmitted power is allocated equally on each hop. The transmitted power at each relay hop, denoted as P_s, is therefore given by

$$P_s = \frac{P_t}{N_r}, \tag{15}$$

where P_t is the total transmitted power. N_r is the number of relay hops, which equals to $N+1$ or $2N$ for the serial or parallel configuration, respectively.

Now consider a FSO hop between two *consecutive* nodes i-th and j-th. The electrical signal after APD detection at the j-th node can be written as

$$r_j = \left[r_j^m, r_j^s\right] = \left[\tfrac{1}{4}m\Re\bar{g}P_s a_{i,j}x_{i,j} + n_j^m, -\tfrac{1}{4}m\Re\bar{g}P_s a_{i,j}x_{i,j} + n_j^s\right], \tag{16}$$

where r_j^m and r_j^s are the received signal in the mark and the space states, respectively. $a_{i,j}$ and $x_{i,j}$ represent the channel loss and the irradiance fluctuation of the hop between nodes i-th and j-th, as in the above analysis. n_j^m and n_j^s denote the receiver noise corresponding to the mark and space states at the j-th node. Note that, n_j^m and n_j^s have the same variance σ_j^2, which is given by

$$\sigma_j^2 = \frac{4k_BT}{R_L}F_n\Delta f + 2q\bar{g}^2F_A\Re\left(\frac{m}{4}P_s a_{i,j}x_{i,j}\right)\Delta f. \tag{17}$$

1) Serial configuration: In serial relaying, the received signal at the j-th node (j = 1, 2, ..., N+ 1) is given by

$$r_j = \left[r_j^m, r_j^s\right] = \left[\tfrac{1}{4}m\Re\bar{g}P_s a_{j-1,j}x_{j-1,j} + n_j^m, -\tfrac{1}{4}m\Re\bar{g}P_s a_{j-1,j}x_{j-1,j} + n_j^s\right]. \tag{18}$$

In this case, the variance of the receiver noises in the mark and space states, n_j^m and n_j^s, is also given as Eq. (17) with $i = j-1$.

2) Parallel configuration: In this case, the source transmits signal to each relay node directly. The received signal at the j-th relay node ($j = 1, 2, ..., N$) is therefore given by

$$r_j = \left[r_j^m, r_j^s\right] = \left[\tfrac{1}{4}m\Re\bar{g}P_s a_{0,j}x_{0,j} + n_j^m, -\tfrac{1}{4}m\Re\bar{g}P_s a_{0,j}x_{0,j} + n_j^s\right]. \tag{19}$$

The noise variance of n_j^m and n_j^s is given as Eq. (17) with $i = 0$. In the parallel relaying, the system can operate even when not all of the relay nodes successfully decode the received signal. Denote S

as the *decoded set*, which is the set of relay nodes that decode the received signal successfully. The received signal at the destination thus can be obtained by adding individuals transmitted signal from the decoded set as

$$r_{N+1} = \left[r^m_{N+1}, r^s_{N+1}\right] \quad = \left[\tfrac{1}{4}m\Re\bar{g}P_s\sum_{i\in \mathrm{S}}(a_{i,N+1}x_{i,N+1}) + n^m_{N+1}, -\tfrac{1}{4}m\Re\bar{g}P_s\sum_{i\in \mathrm{S}}(a_{i,N+1}x_{i,N+1}) + n^s_{N+1}\right]. \tag{20}$$

The variance of the receiver noise at the destination in the mark and space states, denoted as σ^2_{N+1}, therefore can be derived as

$$\sigma^2_{N+1} = \frac{4k_BT}{R_L}F_n\Delta f + 2q\bar{g}^2F_A\Re\big(\frac{m}{4}P_s\sum_{i\in \mathrm{S}}a_{i,N+1}x_{i,N+1}\big)\Delta f. \tag{21}$$

III. Outage Analysis

In the proposed ADF systems, all relay nodes decode the received signal before regenerating and forwarding it to the next one, the calculation of outage probability at each intermediate hop is necessary. For each hop, outage is defined as state at which signal cannot be decoded with an arbitrarily low error probability for a given bit rate, e.g., R_b; in other words, the outage happens when the instantaneous signal-to-noise ratio (SNR) falls bellow a threshold value, denoted as γ_{th}, at which the equivalent instantaneous capacity is equal to R_b. In this paper, we assume that the same γ_{th} value is applied for all hops. When outage happens, the corresponding node is failed and it will stop forwarding signal to the next one. For a BPSK/FSO link, the outage probability of the link can be expressed as

$$P_{out}(\gamma) = \Pr(\gamma < \gamma_{th}). \tag{22}$$

Here, γ is the instantaneous electrical SNR at the receiver, which can be given as

$$\gamma = \frac{(\mu^m - \mu^s)^2}{2\sigma^2}, \tag{23}$$

where σ^2 is the noise variance of receiver noise, μ^m and μ^s are the means of the received signal at the mark and space states as mentioned in Eq. (11), respectively.

From Eqs. (16), (17) and (23), the SNR of the hop between two consecutive nodes i-th and j-th can be expressed by

$$\gamma_{i,j} = \frac{(m\Re\bar{g}P_sa_{i,j}x_{i,j})^2}{8\sigma^2_j}. \tag{24}$$

By denoting $\mathrm{F}_X(x)$ as the cumulative distribution function (cdf) of the random variable X, outage probability of this hop can be expressed as

$$P^{hop}_{out}(\gamma_{i,j}) = \mathrm{F}_X\left(\frac{4N_r\gamma_{th}C + \sqrt{\Delta}}{Aa_{i,j}}\right), \tag{25}$$

where Δ is defined by

$$\Delta = \Big(4N_r\gamma_{th}C\Big)^2 + 8N_r^2\gamma_{th}BA. \tag{26}$$

In these Eqs. (25) and (26), A, B and C are defined in Appendix A. The proof of Eq. (25) derivation also can be found in this Appendix.

A. Serial Configuration

In the serial relaying, an outage occurs if any one of the intermediate links breaks down. The outage probability of the system therefore can be given by

$$P_{out} = \Pr\Big(\bigcup_{j=1}^{N+1}\{\gamma_{j-1,j} < \gamma_{th}\}\Big) = 1 - \Pr\Big(\bigcap_{j=1}^{N+1}\{\gamma_{j-1,j} > \gamma_{th}\}\Big) = 1 - \prod_{j=1}^{N+1}\Big[1 - P_{out}^{hop}(\gamma_{j-1,j})\Big]. \quad (27)$$

Inserting Eq. (25) into Eq. (27) yields

$$P_{out} = 1 - \prod_{j=1}^{N+1}\left[1 - \mathrm{F}_X\left(\frac{4(N+1)\gamma_{th}C + \sqrt{\Delta_s}}{Aa_{j-1,j}}\right)\right], \quad (28)$$

where Δ_s is given by Eq. (26) as $N_r = N+1$ for the case of serial relaying.

1) Log-normal channel: In case of log-normal channel, Eq. (28) can be rewritten as

$$P_{out} = 1 - \prod_{j=1}^{N+1}\left[1 - Q\left(\frac{\ln\left(\frac{Aa_{j-1,j}}{4(N+1)\gamma_{th}C+\sqrt{\Delta_s}}\right)}{\sigma_s^{(j-1)}} - \frac{\sigma_s^{(j-1)}}{2}\right)\right], \quad (29)$$

where $\sigma_s^{(j-1)}$ is the deviation of atmospheric turbulence of the hop connecting the $(j-1)$- th and j-th relay nodes. $Q(x) = \frac{1}{\sqrt{2\pi}}\int_x^\infty \exp\left(-\frac{t^2}{2}\right)\mathrm{d}t$ is the Gaussian Q-function.

2) Gamma-gamma channel: The cdf of the gamma-gamma distribution with two parameters α, β defined in Eqs. (7) and (8) is given by [11]

$$\mathrm{F}_X(x) = \frac{(\alpha\beta x)^{\frac{\alpha+\beta}{2}}}{\Gamma(\alpha)\Gamma(\beta)}\mathrm{G}_{1\,3}^{2\,1}\left(\begin{matrix}1-\frac{\alpha+\beta}{2}\\ \frac{\alpha-\beta}{2},\frac{\beta-\alpha}{2},-\frac{\alpha+\beta}{2}\end{matrix}\middle|\alpha\beta x\right), \quad (30)$$

where $\mathrm{G}_{p,q}^{m,n}[.]$ is the Meijer's G-function [17].

By substituting Eq. (30) into Eq. (28), the closed-form expression of the outage probability P_{out} can be derived.

B. Parallel Configuration

In the parallel relaying, the outage occurs in one of the hops between the source and relay hops may not result in an outage of the system. In this case, an outage happens when either the decoded set S is empty or the MISO (multiple-input single-output) link between the relay nodes and the destination fails. From Eqs. (20) and (21), the SNR at the destination can be derived as

$$\gamma_S = \frac{\left(m\Re\bar{g}P_s\sum_{i\in\mathrm{S}}a_{i,N+1}x_{i,N+1}\right)^2}{8\sigma_{N+1}^2}. \quad (31)$$

Making the change of random variable $z_S = \sum_{i\in\mathrm{S}}a_{i,N+1}x_{i,N+1}$ and using the definitions of A, B and C, the outage probability of this MISO link can be given by

$$P_{out}^{MISO}(\gamma_S) = \mathrm{F}_{Z_S}\left(\frac{4(2N)\gamma_{th}C + \sqrt{\Delta_p}}{A}\right), \quad (32)$$

where $\mathrm{F}_{Z_S}(.)$ is the cdf of random variable z_s, Δ_p is defined as Eq. (26) as $N_r = 2N$ for the case of parallel relaying.

Note that there are 2^N possibilities of decoded set. We denote $\mathrm{W_n}$ as the n-th set and let $\Pr(\mathrm{W_n})$ be the probability of the event $\{\mathrm{S} = \mathrm{W_n}\}$. The outage probability of the system can be expressed as

$$P_{out} = \sum_{n=1}^{2^N} P_{out}^{MISO}(\gamma_{\mathrm{W_n}}) \Pr(\mathrm{W_n}). \tag{33}$$

Assuming that the j-th relay node belongs to $\mathrm{W_n}$, implying that no outage between the source and j-th node. We therefore have $\Pr(j \in \mathrm{W_n}) = 1 - P_{out}^{hop}(\gamma_{0,j})$, where $P_{out}^{hop}(\gamma_{0,j})$ is the outage probability of the j-th hop, which is given in Eq. (25).

For the j-th relay node, which does not belong to $\mathrm{W_n}$, obviously, we have $\Pr(j \notin \mathrm{W_n}) = P_{out}^{hop}(\gamma_{0,j})$. As a result, we could obtain

$$\Pr(\mathrm{W_n}) = \prod_{j \in \mathrm{W_n}} \left(1 - P_{out}^{hop}(\gamma_{0,j})\right) \times \prod_{j \notin \mathrm{W_n}} P_{out}^{hop}(\gamma_{0,j}) \tag{34}$$

By substituting Eqs. (32), (34) into Eq. (33), the outage probability of the parallel relaying can be expressed as

$$\begin{aligned} P_{out} = \sum_{n=1}^{2^N} \Bigg[\prod_{j \in \mathrm{W_n}} \left(1 - \mathrm{F}_X\left(\frac{4(2N)\gamma_{th}C + \sqrt{\Delta_p}}{Aa_{0,j}}\right)\right) \times \prod_{j \notin \mathrm{W_n}} \mathrm{F}_X\left(\frac{4(2N)\gamma_{th}C + \sqrt{\Delta_p}}{Aa_{0,j}}\right) \Bigg] \\ \times \mathrm{F}_{z_{\mathrm{W_n}}}\left(\frac{4(2N)\gamma_{th}C + \sqrt{\Delta_p}}{A}\right). \end{aligned} \tag{35}$$

1) Log-normal Channel: In case X is the log-normal distribution, the exact distribution of z_s is unknown. However, there have been several methods for approximating the sum of log-normal random variables [18], [19]. In this study, we employ the well-known Fenton-Wilkinson method [20], in which, the approximated logarithm mean μ_{z_S} and logarithm variance $\sigma_{z_S}^2$ of z_s can be derived as

$$\mu_{z_S} = \ln \sum_{i \in \mathrm{S}} a_{i,N+1} - \frac{\sigma_{z_S}^2}{2}, \tag{36}$$

$$\sigma_{z_S}^2 = \ln\left[1 + \frac{\sum_{i \in \mathrm{S}} a_{i,N+1}^2 \left(e^{\sigma_s^2(\ell_{i,N+1})} - 1\right)}{\left(\sum_{i \in \mathrm{S}} a_{i,N+1}\right)^2}\right]. \tag{37}$$

Therefore, the approximation of the outage probability can be derived as

$$\begin{aligned} P_{out} \approx \sum_{n=1}^{2^N} \Bigg\{ \prod_{j \in \mathrm{W_n}} \left[1 - Q\left(\frac{\ln\left(\frac{Aa_{0,j}}{4(2N)\gamma_{th}C + \sqrt{\Delta_p}}\right)}{\sigma_s^{(j)}} - \frac{\sigma_s^{(j)}}{2}\right)\right] \times \prod_{j \notin \mathrm{W_n}} \left[Q\left(\frac{\ln\left(\frac{Aa_{0,j}}{4(2N)\gamma_{th}C + \sqrt{\Delta_p}}\right)}{\sigma_s^{(j)}} - \frac{\sigma_s^{(j)}}{2}\right)\right] \Bigg\} \\ Q\left(\frac{\ln\left(\frac{A}{4(2N)\gamma_{th}C + \sqrt{\Delta_p}}\right) + \mu_{z_{\mathrm{W_n}}}}{\sigma_{z_{\mathrm{W_n}}}}\right), \end{aligned} \tag{38}$$

where $\sigma_s^{(j)}$ is the deviation of atmospheric turbulence of the hop connecting the source and the j-th relay node.

2) Gamma-gamma Channel: In [21], it is shown that the sum of Gamma-gamma random variables can be approximated efficiently by a Gamma random variable. We will apply this result to approximate the random variable z_S.

Assuming that z_S is approximated by a Gamma random variable Ψ_S, the scale parameter θ_S and shape parameter k_S of Ψ_S are defined by

$$\theta_S = \frac{\sum_{i\in \mathrm{S}} K_{S_i} a_{i,N+1}^2 + 2\sum_{i\in \mathrm{S}} \sum_{\substack{j\in \mathrm{S} \\ j>i}} a_{i,N+1} a_{j,N+1}}{\sum_{i\in \mathrm{S}} a_{i,N+1}} - \sum_{i\in \mathrm{S}} (1+\varepsilon_i) a_{i,N+1}, \tag{39}$$

$$k_S = \frac{\sum_{i\in \mathrm{S}} a_{i,N+1}}{\theta_S}, \tag{40}$$

where K_{S_i} is given by

$$K_{S_i} = 1 + \frac{1}{\alpha^{(i)}} + \frac{1}{\beta^{(i)}} + \frac{1}{\alpha^{(i)}\beta^{(i)}}, \tag{41}$$

where $\alpha^{(i)}$, $\beta^{(i)}$ are the parameters of Gamma-gamma distribution for atmospheric turbulence of the hop connecting the i-th relay node and the destination.

The adjustment parameters $\{\varepsilon_i\}$ can be chosen in the range $[-\infty; K_{S_i} - 1]$. The outage probability of the MISO link therefore can be derived as

$$P_{out}^{MISO}(\gamma_S) \approx \frac{1}{\Gamma(k_S)} \Phi\left(k_S, \left(\frac{4(2N)\gamma_{th}C + \sqrt{\Delta_p}}{A\theta_S}\right)\right), \tag{42}$$

where $\Phi(w,x) = \int_0^x e^{-t} t^{w-1} \mathrm{d}t$ is the lower incomplete gamma function.

By integrating Eqs. (30), (42) into Eq. (35), we have the closed-form expression that approximates the outage probability for the case of the parallel relaying.

IV. Numerical Results & Discussions

For analytical results and simulation, the turbulence strength C_n^2 is set to 8×10^{-15} for log-normal channel and 3×10^{-14} for gamma-gamma channel, and the distance from the source to the destination is $L = 2$ km. In the serial configuration, the distances between any two consecutive nodes are assumed to be equal. In the parallel configuration, the relay nodes are placed on the halfway point, i.e., the point at which the distances from the source to relay nodes and from relay nodes to the destination are the same. Also, for the sake of simplicity, we assume that these distances are equal $L/2$.

For the FSO link, the atmospheric extinction coefficient $\beta_\nu = 0.1$ dB/km, the diameter of the receiver's aperture $D = 0.03$ m, the angle of divergence is chosen to be 10^{-3} radian and SNR threshold value is 0 dBm. Unless otherwise noted, we use the system bit rate $R_b = 2$ Gb/s, the receiver noise temperature $T = 300$ K and the optical wavelength $\lambda = 1550$ nm. Other system parameters are: the modulation index $m = 1$, the APD responsitivy $\Re = 1$, the APD load resistance $R_L = 1000\ \Omega$, the amplifier noise figure $F_n = 2$, and the ionisation factor $k_A = 0.7$ for a typical InGaAs APD. Furthermore, for a fair comparison between different systems with different configurations and different numbers

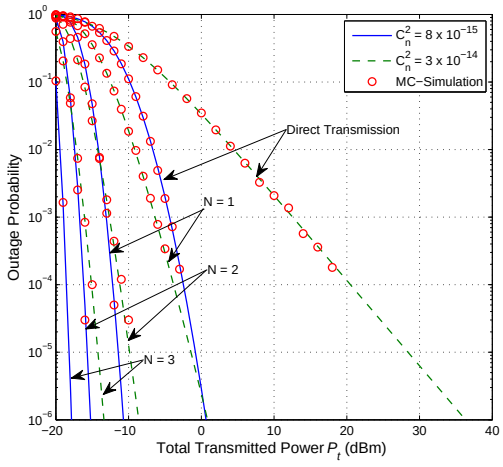

Fig. 3: Outage probability versus total transmitted power P_t in cases of log-normal and gamma-gamma channels and $\bar{g} = 35$. Analytical and Monte Carlo simulation results.

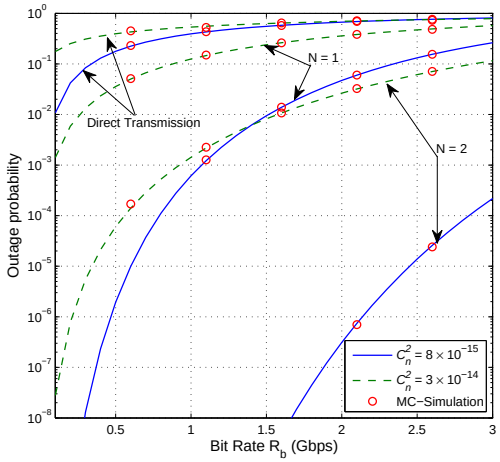

Fig. 4: Outage probability versus bit rate with $P_t = -15$ dBm, $\bar{g}$ = 35 for different numbers of relay nodes and turbulence strengths.

of relay nodes, we analyse the outage probability under a constraint on the total transmitted power, i.e., as the number of relays increases, power allocated to each hop will be decreased accordingly.

A. Serial Configuration

Figure 3 shows the outage probability of serial relaying versus the total transmitted power for both log-normal and gamma-gamma channels with different numbers of relay nodes. The average APD gain is set to 35. It is observed that an increase in the number of relay nodes results in a better

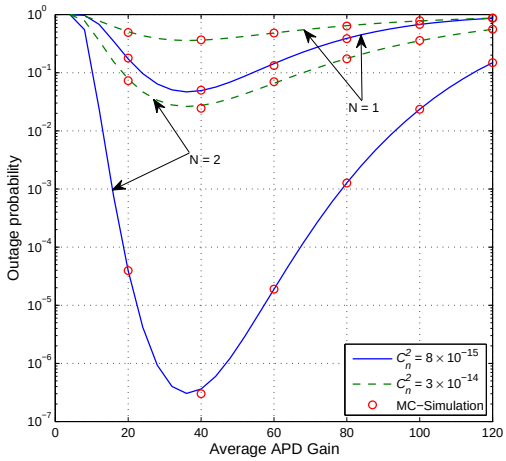

Fig. 5: Outage probability versus average APD gain for log-normal and gamma-gamma channels when $P_t = -15$ dBm for different numbers of relay nodes and turbulence strengths

performance, i.e., lower outage probability, in both cases of atmospheric turbulence channels. In case of log-normal channel, at the outage probability of 10^{-6}, the power gain compared to direct transmission, when the numbers of relay nodes $N = 1, 2,$ and 3, are 12 dB, 16 dB, and 19 dB, respectively. In case of gamma-gamma channel, the improvements are 35 dB, 44 dB, and 50 dB for $N = 1, 2$, and 3, respectively. Monte Carlo simulations are also used to verify the analytical results and the good agreement between the simulation and analytical results for both turbulence channel models confirms the validity of the analysis.

In Fig. 4, the outage probability is represented with respect to the system bit rate for different numbers of relay nodes. The total transmitted power is fixed at -15 dBm and the average APD gain of 35 is selected. It is seen that the relay transmission could significantly increase the system bit rate. For example, at the outage probability of 10^{-6} with turbulence strength $C_n^2 = 8 \times 10^{-15}$, the 2-node relaying system could support the bit rate of higher than 2.2 Gbps while it is not able to do so with the direct or 1-node relaying system. It is also seen that the outage probability is getting worse drastically as the bit rate increases, especially in the strong turbulence conditions. For example, when $N = 1$ and $C_n^2 = 8 \times 10^{-15}$, the outage probability goes up from 10^{-6} to 10^{-2} when bit rate increases from 0.5 Gbps to 1.5 Gbps.

Figure 5 demonstrates the relationship between the outage probability and the average APD gain with two values of turbulence strength corresponding to the log-normal and gamma-gamma channels. Obviously, the system outage performance is greatly improved as the number of relay nodes increases. In addition, we also see that, similar to the case of single hop, the performance of the multihop system can also be optimised by selecting an appropriate value of APD gain. Furthermore, the optimal gain,

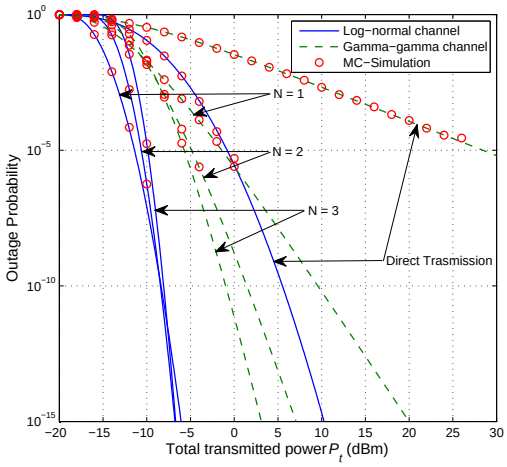

Fig. 6: Outage probability versus total transmitted power in cases of log-normal and gamma-gamma channels when $\bar{g} = 35$. Analytical and Monte Carlo simulation results.

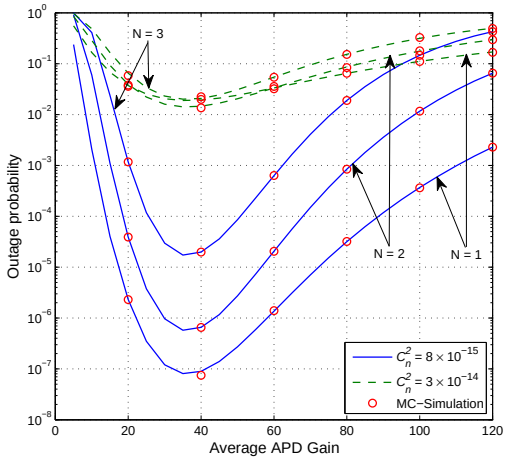

Fig. 7: Outage probability versus average APD gain when $P_t = -10$ dBm for different turbulence strengths and numbers of relay nodes.

under the assumption of the same APD receiver for all nodes, is almost unchanged for different numbers of nodes and it is close to 38 in case of InGaAs APD receiver in both of log-normal and gamma-gamma channels. This is because of two reasons. This is because the value of optimal gain is mainly determined by APD parameters, especially the exceed noise factor F_A [16].

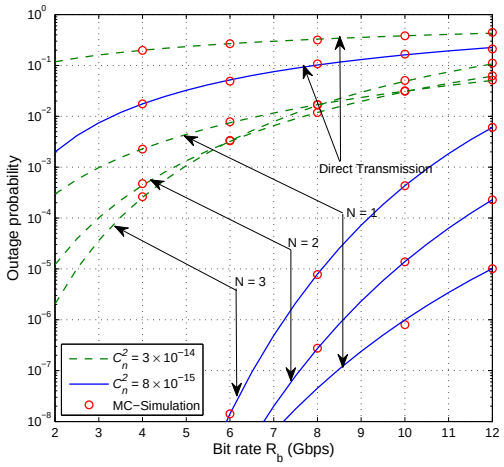

Fig. 8: Outage probability versus bit rate for different turbulence strengths when $P_t = -5$ dBm, $\bar{g}$ = 35 with different numbers of relay nodes.

B. Parallel Configuration

This section focuses on the outage analysis for the parallel configuration. Figure 6 shows the outage probability of the parallel relaying system versus the total transmitted power for log-normal and gamma-gamma channels. Similar to the case of serial configuration, the analytical results are also confirmed by the Monte Carlo simulations. It is seen that using the multihop system also improves the outage performance. However, unlike the serial relaying, the increase of the number of relay nodes in the parallel system does not always result in better performance. In particular, when the total transmitted power is smaller than -7 dBm in case of log-normal channel, at the outage probability of 10^{-6}, when N increases from 1 to 2 then 3, the additional required transmitted powers are about 1 dB for each increase. The improvement when N increases can be seen again when the total transmitted power is high enough.

This result is logical as when N increases, the transmitted power for each hop is deceased. However, unlike the serial relaying, the increase of N does not result in shorter transmission distance of a hop (and it is the same as $L/2$). As a result, when the total transmitted power is not high, the increase of N results in worse outage performance in each hop, especially the hops from the source to the relay nodes. Consequently, the overall performance of the system is degraded. It is therefore recommended that for parallel relaying, the number of relay nodes should not be higher than 3. In addition, when the total transmitted power is limited the serial relaying is more favourable, especially in the presence of strong turbulence.

Next, we consider the impact of the number of relay nodes on the selection of the optimal APD gain for log-normal and gamma-gamma channels in Fig. 7. We also assume that the APD receivers at the

destination and relays nodes have the same parameters. Again, it is confirmed that the increase in the number of relay nodes does not result in the performance improvement in case of weak turbulence, as shown in Fig. 6. In addition, with the similar reason to that of the serial configuration, the optimal gain is almost the same for different systems with different numbers of relays.

Finally, in Fig. 8, we investigate the maximum bit rate at a given outage probability for different turbulence strengths. The total transmitted power $P_t = -5$ dBm is set, average APD gain $\bar{g} = 35$ and the number of relay nodes is from 1 to 3. It is also seen that the outage performance is greatly improved in the multihop systems, especially in case of weak turbulence. In addition, similar to serial relaying systems, the increase of the number of relay nodes results in the higher outage probability when the turbulence is weak (i.e. $C_n^2 = 8 \times 10^{-15}$ in this figure). In case of strong turbulence, it is seen that the outage probability is improved as the number of relay nodes increases.

V. Conclusions

We have proposed and analysed the performance of ADF multihop FSO systems using the subcarrier BPSK signalling and APD receivers for serial and parallel configurations over both log-normal and gamma-gamma turbulence channels. The closed-form expressions of the outage probability were analytically derived taking into account both the atmospheric turbulence and the receiver noise, which includes the APD shot noise and thermal noise. The analytical results were confirmed by Monte Carlo simulations. It was seen that the outage performance was significantly improved in both relaying configurations in comparison with that of the direct transmission. In the parallel relaying however, the increase in the number of relay nodes did not always result in the better performance, especially when the total transmitted power is low. The serial relaying was thus more favourable; and with a proper selection of the number of relay nodes, good outage performance could be achieved at relatively low powers, even in the presence of strong turbulence. The selection of the APD gain also greatly affected the outage probability of the system; however, it was found that the optimal APD gain was almost unchanged in both relaying configurations with different number of relays.

Appendix A
Proof of Equation (25)

Let's define $A = (m\Re\bar{g}P_t)^2$, $B = \frac{4k_BT}{R_L}F_n\Delta f$, $C = 2q\bar{g}^2F_A\Re\left(\frac{m}{4}P_t\right)\Delta f$ and replace $P_s = \frac{P_t}{N_r}$ into Eq. (24), it can be re-written as

$$\gamma_{i,j} = \frac{Aa_{i,j}^2x_{i,j}^2}{8N_r^2B + 8N_rCa_{i,j}x_{i,j}}. \tag{43}$$

Replacing $\gamma_{i,j}$ into Eq. (22), the outage probability of the relay hop between nodes i-th and j-th can be expressed as

$$P_{out}^{hop}(\gamma_{i,j}) = \Pr\left(x_{i,j} < \frac{4N_r\gamma_{th}C + \sqrt{\Delta}}{Aa_{i,j}}\right). \tag{44}$$

The outage probability of the hop can be therefore derived as in Eq. (25)

REFERENCES

[1] Willebrand, H., Ghuman, B.S. :'Free-Space Optics: Enabling Optical Connectivity in Today's Networks', (Sams Publishing., 2001)

[2] Ghassemlooy, Z., Popoola, W.O., and Rajbhandari, S.: 'Optical Wireless Communications System and Channel Modelling with Matlab', (CRC publisher, USA, August 2012, ISBN: 978-4398-5188-3).

[3] ElBatt, T., Izadpanal, H.: 'Design aspects of hybrid RF/ free space optical wireless networks', *IEEE BroadBand Communications for the Internet Era Symposium*, 2001, pp. 157–161.

[4] Acampora, A.S., Krishnamurthy, S.V.: 'A broadband wireless access network based on mesh-connected free-space optical links', *Personal Communications, IEEE*, 1991, **6**, (5), pp.62–65.

[5] Safari, M., Uysal, M.: 'Relay-assisted free-space optical communication', *IEEE Trans. Commun.*, 2008, **7**, (12), pp. 5441–5449.

[6] Karimi, M., Nasiri-Kenari, M.: 'Outage analysis of relay-assisted free-space optical communications', *IET Commun.*, 2010, **4**, (12), pp. 1423–1432.

[7] Datsikas, C.K., Peppas, K.P., Sagias, N.C., Tombras, G.S.: 'Serial Free-Space Optical Relaying Communications Over Gamma-Gamma Atmospheric Turbulence Channels', *IEEE/OSA J. of Opt. Commun. and Netw.*, 2010, **2**, (8), pp.576–586.

[8] Bhatnagar, M.R.: 'Performance Analysis of Decode-and-Forward Relaying in Gamma-Gamma Fading Channels', *IEEE Photonics Technology*, 2012, **24**, (7), pp.545–547.

[9] Tsiftsis, T.A., Sandalidis, H.G., Karagiannidis, G.K., Sagias, N.C.: 'Multihop Free-Space Optical Communications over Strong Turbulence Channels', Communications, 2006. ICC'06. IEEE International Conference on, **6**, page. 2755–2759.

[10] Bayaki, E., Michalopoulos, D.S., Schober, R.: 'EDFA-Based All-Optical Relaying in Free-Space Optical Systems', *IEEE Trans. Commun.*, 2012, **60**, (12), pp. 3797–3807.

[11] Nistazalis, H. E., Tsiftis, T. A., Tombras, G. S.: 'Performance analysis of free-space optical communication systems over atmospheric turbulence channels', *IET Commun.*, 2009, **3**, (8), pp. 1402–1409.

[12] Kiasaleh, K.: 'Performance of APD-based, PPM free-space optical communication systems in atmospheric turbulence', *IEEE Trans. Commun.*, 2005, **53**, (9), pp. 1455–1461.

[13] Duy A. Luong, T.C. Thang and Anh T. Pham: 'Effect of avalanche photodiode and thermal noises on the performance of binary phase-shift keying subcarrier-intensity modulation/free-space optical systems over turbulence channels', *IET Commun.*, 2013, **7**, (8), pp. 738–744.

[14] Karp, S.: 'Optical channels: fibers, clouds, water and the atmosphere' (Plenum Press, 1998).

[15] Al Habash, M. A., Andrews, L. C., Phillips, R. L.: 'Mathematical model for the irradiance probability density function of a laser beam propagating through turbulent media', *Opt. Eng.*, 2001, **40**, (8), pp. 1554–1562.

[16] Agrawal, G.P.: 'Fiber-Optic Communication Systems' (John Wiley & Sons Inc, 2002, 3rd edition).

[17] Gradshteyn, I. S., Ryzhik. I. M.: 'Table of integrals, series, and products,' (Academic Press, 2007, 7th edition).

[18] Norman C.Beaulieu, Adnan A.Abu-Dayya, and Peter J. McLane.: 'Estimating the distribution of a sum of independent lognormal random variables', *IEEE Trans. Commun.*, 1995, **43**, (12), pp. 2869–2873.

[19] Janos, W.: 'Tail of the distribution of sums of log-normal variates', *IEEE Trans. Commun.*, 1970, **16**, (3), pp. 299–302.

[20] Fenton, L.: 'The Sum of Log-Normal Probability Distributions in Scatter Transmission Systems', *IRE Trans.*, 1960, **8**, (1), pp. 57–67.

[21] Al-Ahmadi, S., Yanikomeroglu, H.: 'On the Approximation of the Generalized-K PDF by a Gamma PDF Using the Moment Matching Method', Wireless Communications and Networking Conference (WCNC), 2009, pp. 1–6.

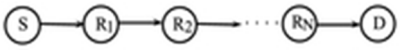

16x2mm (300 x 300 DPI)

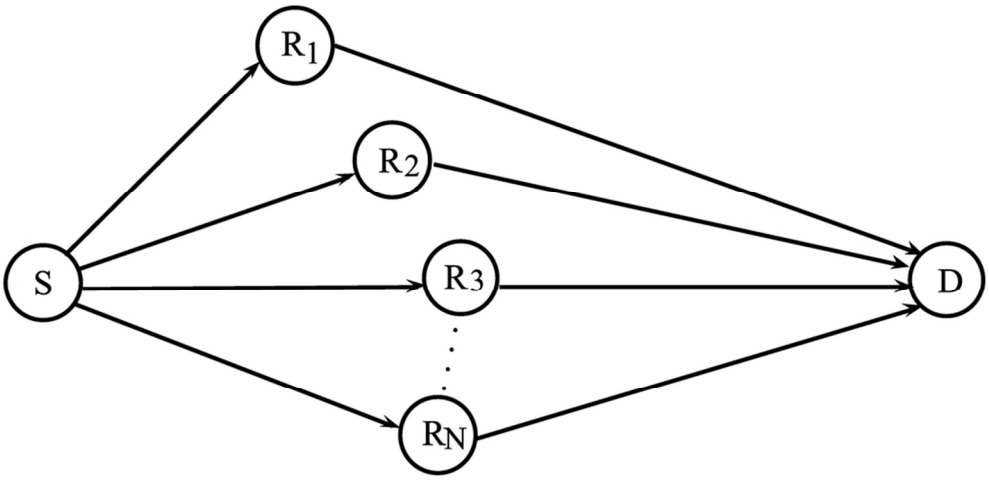

87x42mm (300 x 300 DPI)

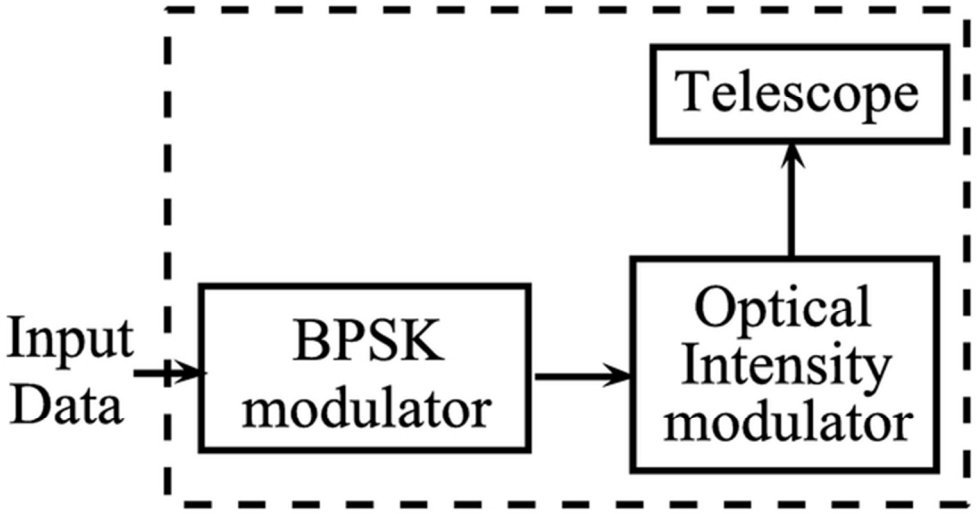

56x29mm (300 x 300 DPI)

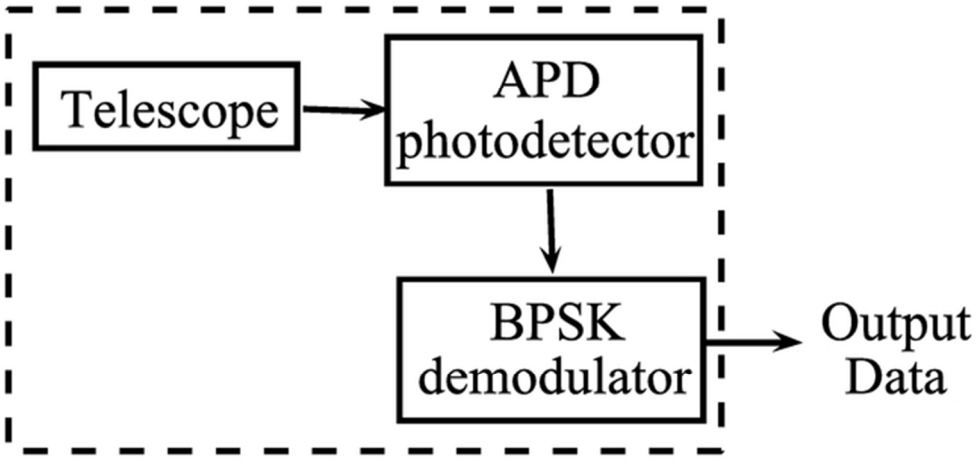

56x26mm (300 x 300 DPI)

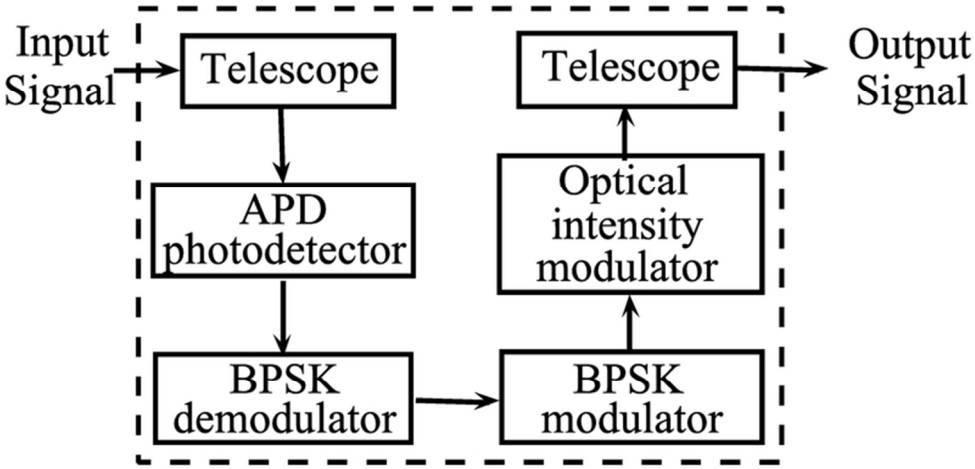

69x33mm (300 x 300 DPI)

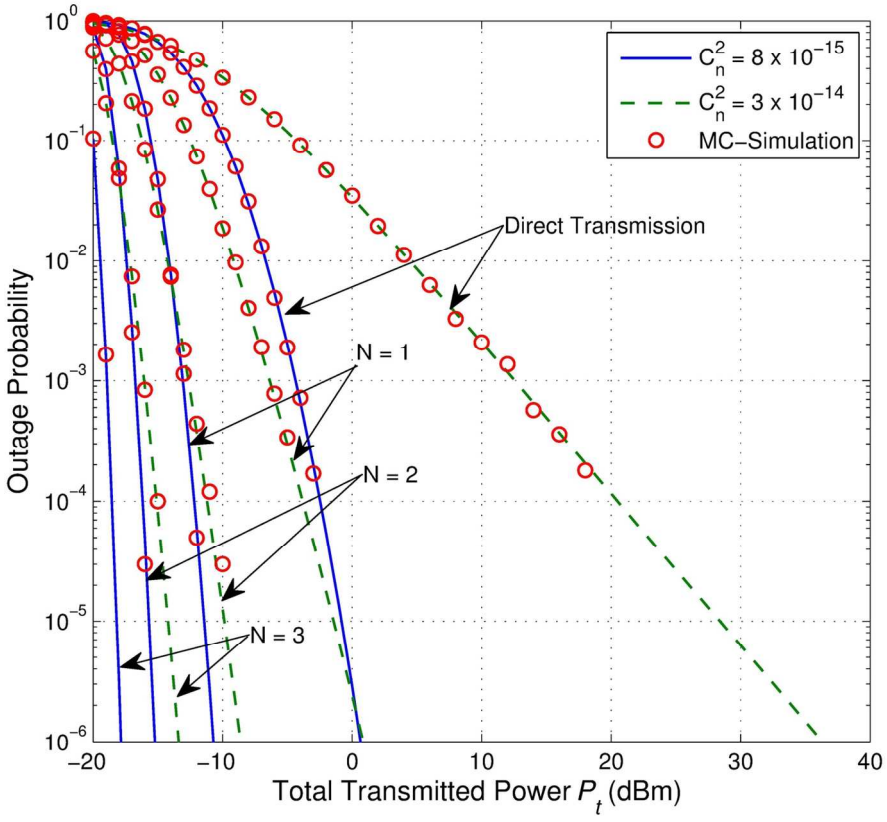

136x121mm (300 x 300 DPI)

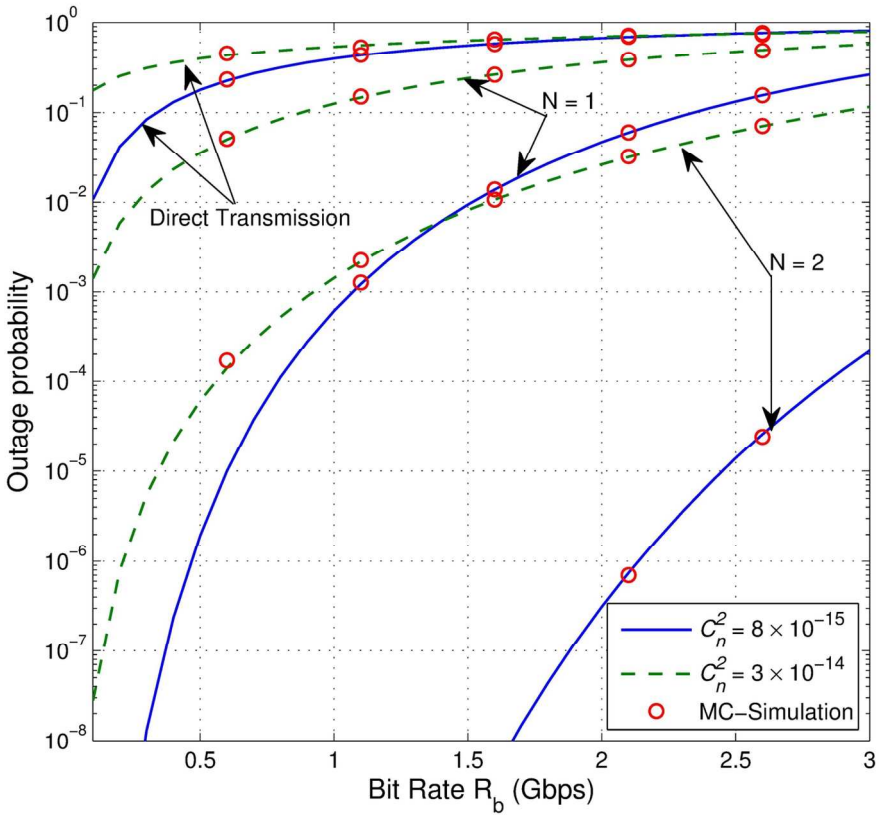

136x120mm (300 x 300 DPI)

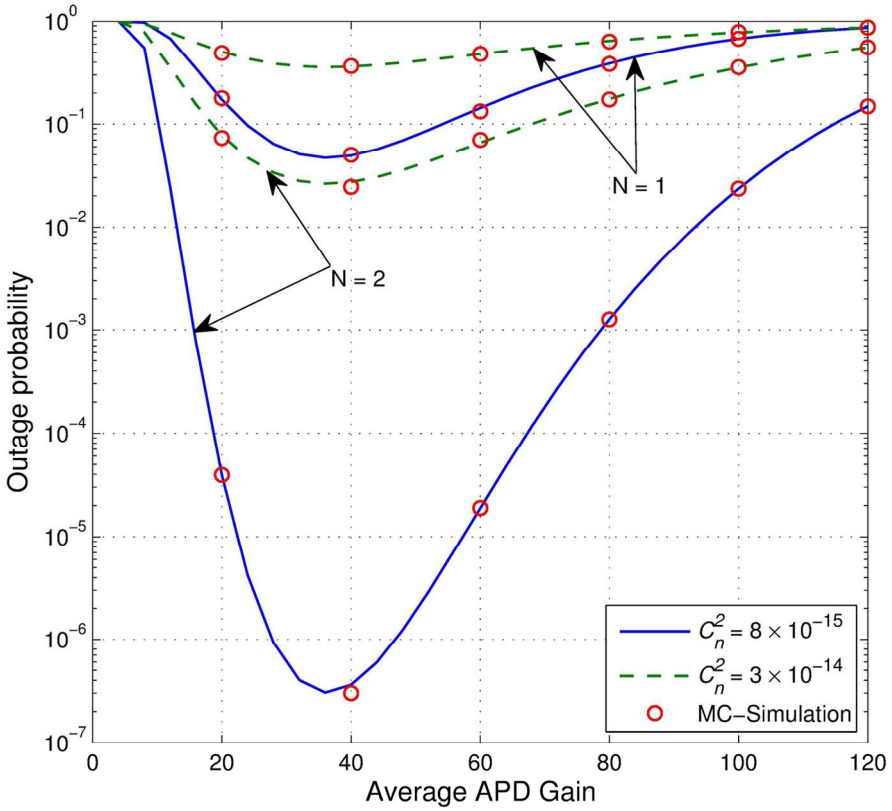

137x121mm (300 x 300 DPI)

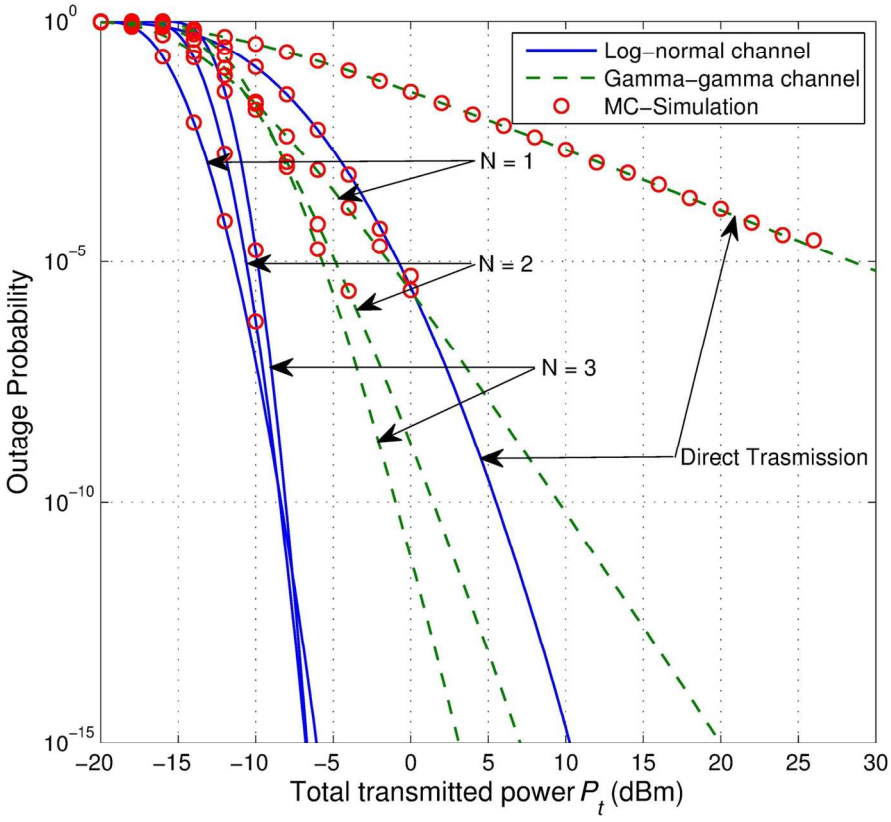

137x121mm (300 x 300 DPI)

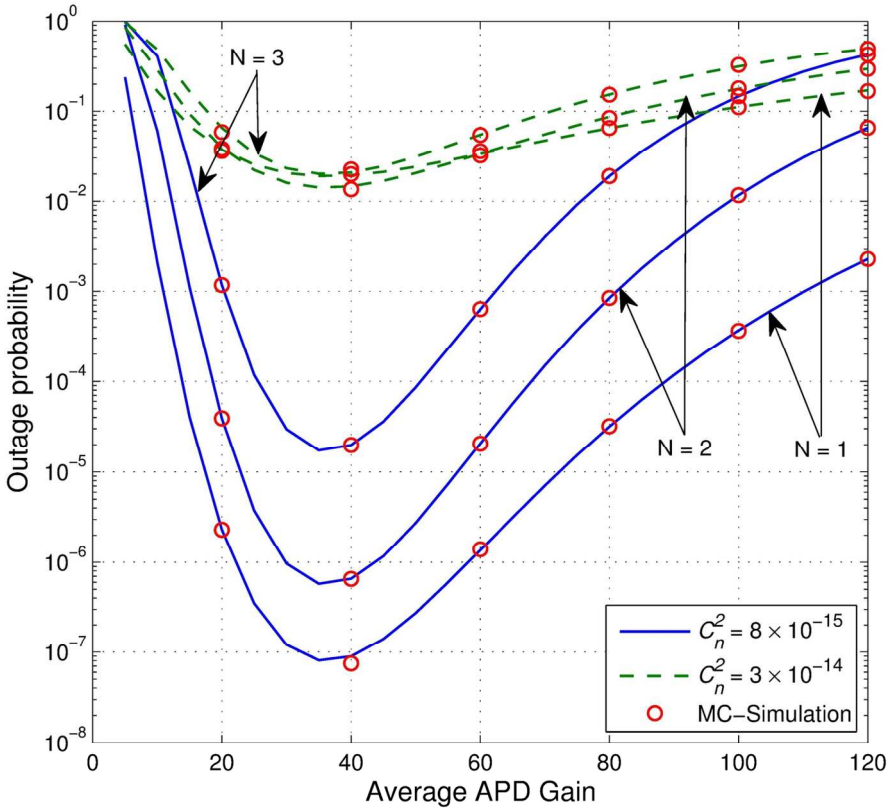

137x121mm (300 x 300 DPI)

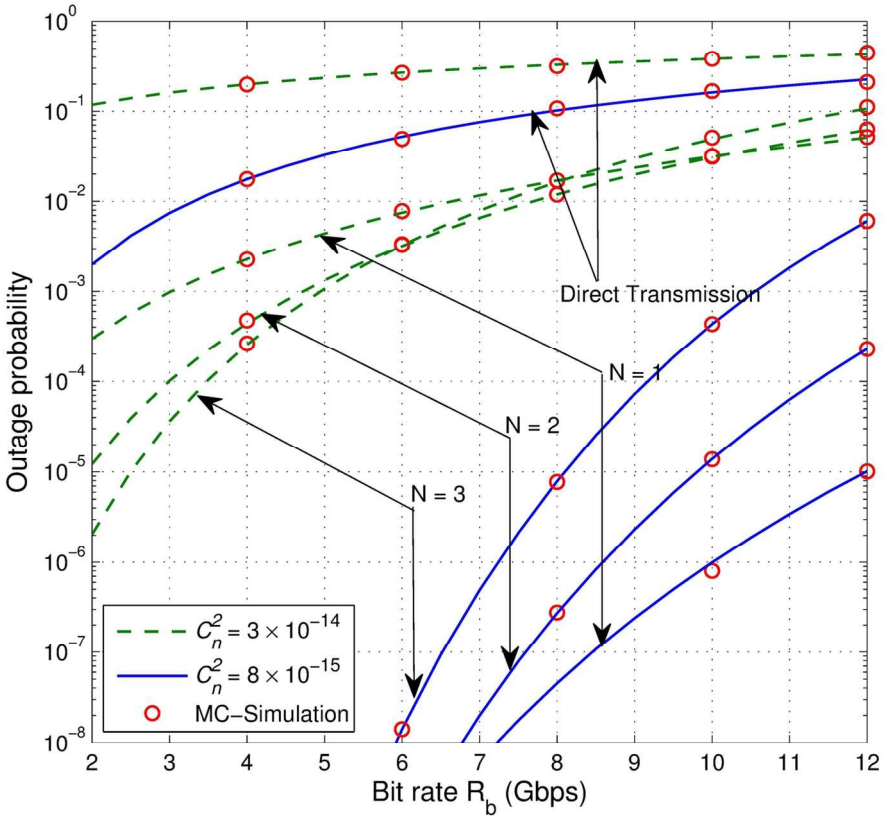

137x121mm (300 x 300 DPI)